



## Structure Reactivity Correlations of Azo Reactive Dyes Based on H-acid. I. NMR Chemical Shift Values, pKa Values, Dyestuff Aggregation and Dyeing Behaviour<sup>1</sup>

Karl Brederbeck\* & Christian Schumacher

Institut für Textil- und Faserchemie, Universität Stuttgart,  
Pfaffenwaldring 55, 7000 Stuttgart 80, Germany

(Received 5 August 1992; accepted 14 September 1992)

### ABSTRACT

*In this series of papers we report on structure reactivity correlations with respect to the degradation of dyestuffs. For this purpose a series of monoazo vinylsulphone/monochlorotriazine reactive dyes, based on H-acid with systematically varied substituents, was investigated in aqueous solution as well as on cellulosic substrates. In the first part we discuss the selected dyes, their synthesis, characterization, dyeing behaviour and some features which are pertinent to an understanding of the fading reactions, namely, the pKa values of the dyes and their aggregation behaviour.*

### 1 INTRODUCTION

Cellulosic fibres are the most important class of fibres worldwide, and the consumption of dyestuffs is of great economic relevance. Among the dye classes which can be applied to cellulosic fibres, for which vat dyes, direct dyes and reactive dyes are the most important ones, the demand for reactive dyes is steadily growing. Their key properties are excellent wet fastness, brilliant shades and simple application techniques. With the increasing economic relevance of this dye class, the requirements for the

\* To whom correspondence should be addressed.

dyes also grew, especially with respect to the fixation yields in exhaustion-dyeing and to the improvement of certain fastness properties. The fading of dyed fabrics by chlorinated water, by laundering with detergents containing peroxide and by the combined action of perspiration and light are considered as major problems in the dyestuff industry.<sup>2</sup> Yet very little is known about the chemistry which is involved in the loss of colour of dyed textiles. Much work has been done pertaining to fastness towards light and washing. However, there is a lack of information about the chemical and physical background concerning the fading caused by chlorine or hypochlorite, peroxide washing and perspiration–light.

The scope of this work was to establish some correlations between the dye structure and its reactivity, with particular respect to the above fastness requirements. For this purpose a series of monoazo reactive dyes, based on H-acid with systematically varied substituents in the diazo moiety (*ortho* and *para* to the azo linkage) and several substituents on the amino group of the H-acid fragment, was synthesized. The dyes were characterized by some selected properties and fundamental aspects relevant to their degradation in solution and on cellulosic substrates were investigated.

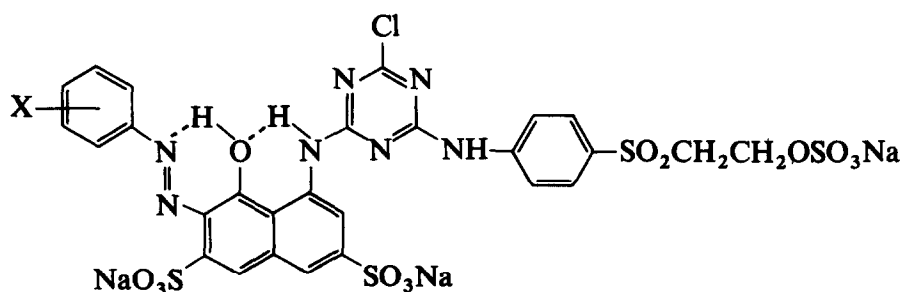
In this first part of a series of papers, some chemical and physical properties of the prepared dyes are discussed. These data are essential for a better understanding of the reactions leading to the degradation of the dyestuffs and to avoid misunderstandings. We report on NMR data, *pK<sub>a</sub>* values, dyestuff aggregation and the dyeing behaviour (substantivity, fixation yields).

## 2 EXPERIMENTAL

### 2.1 Dyes

The investigated dyestuffs were red monoazo dyes based on H-acid with monochlorotriazine (MCT)–vinylsulphone (VS) reactive groups, with both reactive groups located on the same side of the chromophore.

The dyestuffs were prepared according to the usual procedures for cyanuric chloride condensations<sup>3</sup> and azo coupling.<sup>4</sup> In the first step, *p*-( $\beta$ -sulphatoethyl)sulphonylaniline was condensed with cyanuric chloride. This product was then condensed with H-acid in the second step to yield the coupling component. On to this were then coupled the corresponding diazotized aromatic amines. The pH value during the coupling was kept at 7 or below, to maintain the sulphatoethylsulphone (SES) functional group.



X = *p*-OCH<sub>3</sub> (1), *p*-CH<sub>3</sub> (2), H (3), *p*-Cl (4), *p*-NO<sub>2</sub> (5),  
*o*-OCH<sub>3</sub> (6), *o*-CH<sub>3</sub> (7), *o*-Cl (8), *o*-NO<sub>2</sub> (9),  
*o*-SO<sub>3</sub>H (10), *o*-*sec*-C<sub>4</sub>H<sub>9</sub> (11), *o*-COOH (12)

The basic compounds required for the synthesis, H-acid and *p*-( $\beta$ -sulphatoethyl)sulfonylaniline, were supplied by Hoechst AG, Frankfurt am Main, Germany. Cyanuric chloride was purchased from Merck (Darmstadt, Germany). All of the above were used without further purification. The aromatic amines used for the azo couplings were purified by recrystallization from petroleum-ether or by distillation *in vacuo*, respectively.

The dyes were isolated by pouring the aqueous reaction mixture into a 50-fold excess of acetone with vigorous stirring. The dyes precipitated and after 15 min stirring the precipitate was filtered off. All organic impurities were then extracted by washing with small portions of diethyl ether. Further purification was achieved by preparative MPLC, using reversed phase C<sub>18</sub> silica gel (Lobar <sup>®</sup>LiChroprep C<sub>18</sub> from Merck) as

TABLE I  
Elemental Analysis (C, H, N) of the Dyestuffs 1-12

Dye	Calculated				Found				Correction	
	C	H	N	C:N	C	H	N	C:N	H <sub>2</sub> O	NaCl
1	29.57	2.92	8.62	3.43	29.66	2.68	8.32	3.56	6	2
2	32.90	3.45	9.59	3.43	33.02	3.35	9.52	3.47	7	0
3	32.02	2.69	9.68	3.31	32.28	2.72	9.52	3.39	4	1
4	28.41	2.65	8.59	3.31	28.72	2.24	8.19	3.51	6	2
5	31.19	2.33	10.78	2.89	31.13	2.47	10.48	2.97	3	1
6	32.25	2.80	9.40	3.43	32.21	2.85	8.85	3.64	4	1
7	30.49	2.83	8.89	3.43	30.79	2.76	8.56	3.60	5	2
8	29.94	2.79	9.05	3.31	30.04	2.43	8.70	3.45	6	1
9	30.66	2.48	10.59	2.89	30.70	2.55	10.11	3.04	4	1
10	28.63	2.49	8.66	3.31	28.73	2.52	8.55	3.36	5	1
11	36.85	3.49	9.70	3.80	36.81	3.39	9.33	3.95	4	0
12	31.18	2.43	9.09	3.43	31.25	2.54	8.86	3.35	4	1

**TABLE 2**  
 250 MHz FT  $^1\text{H}$ -NMR Chemical Shift Values (ppm) of the Dyestuffs 1–12 in  $d_6$ -DMSO

Dye	NH (s) (hydrazone 1 H)	NH (s) (1 H)	NH (s) (1 H)	—CH <sub>2</sub> — (t) (2 + 2 H)	Aromatic protons	Others
1	16.02	13.05	10.95	3.63; 3.96	7.07–8.00 (10 H); 8.87 (1 H)	3.83 (s, 3 H) O—CH <sub>3</sub>
2	15.81	12.99	10.93	3.59; 3.95	7.29–8.00 (10 H); 8.87 (1 H)	2.51 (s, 3 H) Ar—CH <sub>3</sub>
3	15.60	12.92	10.93	3.62; 3.95	7.24–8.00 (11 H); 8.88 (1 H)	—
4	15.37	12.85	10.95	3.63; 3.97	7.51–8.06 (10 H); 8.86 (1 H)	—
5	15.00	12.64	10.65	3.63; 3.96	7.11–8.34 (10 H); 8.90 (1 H)	—
6	15.84	12.94	10.93	3.59; 3.95	7.09–8.09 (10 H); 8.92 (1 H)	4.04 (s, 3 H) O—CH <sub>3</sub>
7	16.17	13.11	10.93	3.62; 3.97	7.2–8.1 (10 H); 8.95 (1 H)	2.58 (s, 3 H) Ar—CH <sub>3</sub>
8	15.77	12.80	10.92	3.60; 3.94	7.29–8.21 (10 H); 8.93 (1 H)	—
9	16.18	12.89	10.98	3.61; 3.97	7.37–8.61 (10 H); 8.95 (1 H)	—
10	15.80	13.10	10.95	3.65; 3.93	7.18–8.32 (10 H); 8.94 (1 H)	—
11	16.18	13.00	10.90	3.62; 3.96	7.2–8.2 (10 H); 8.82 (1 H)	0.9–1.8 9H mult.
12	16.60	13.35	10.96	?; 3.95	7.17–8.38 (10 H); 8.88 (1 H)	—

(s)—singlet; (t)—triplet; mult.—multiplet; ?—hidden by water peak.

stationary phase, and a water/methanol gradient (0 to 30% methanol) as mobile phase. A careful purification of the dyes is required since impurities significantly affect the degradation reactions (see Part II). The products thus obtained contained only dye, some water and in some cases trace amounts of salt (Table 1).

All elemental analyses (Table 1) and  $^1\text{H}$ -NMR spectra measurements (Table 2) for characterization (250 MHz Fourier transform (FT) NMR spectrometer, in  $d_6$ -DMSO) were carried out at the Institut für Organische Chemie, Universität Stuttgart.

## 2.2 Dyeing

The dyeing of cotton fabric was performed at a goods-to-liquor ratio of 1 : 20 (2% o.w.f.) and a constant temperature of 60°C (isothermic) in a

two-step exhaustion process (step 1: 60 min, neutral dyeing with 50 g/litre sodium chloride; step 2: 90 min, dyeing with 20 g/litre sodium carbonate).

The terms used to characterize the dyeing were the primary exhaustion (percentage of dye adsorbed on to the fibre during dyeing at neutral pH), the secondary exhaustion (dye chemically bound and adsorbed at the end of the dyeing), the fixation yield (dye chemically bound) and the relative fixation yield (dye chemically bound relative to the secondary exhaustion). The relative yield tells us how much dye is chemically fixed when it was already adsorbed on to the fibre.

The experimental procedure was as follows: To 50 ml of demineralized water was added 2.5 g of sodium chloride and 50 mg of the dyestuff. After dissolving, a small sample (1 ml) of the dyebath was collected (sample 1). To the main solution was then added 2.5 g of small pieces of cotton fabric (6 cm × 3 cm each); and the dyeing temperature was quickly raised to 60°C by putting the dyeing vessels into a preheated shaking thermostat. After 60 min of dyeing under vigorous shaking a second sample of 1 ml was taken from the dyebath (sample 2) and 1 g of sodium carbonate was added. The dyeing was then continued for another 90 min. At the end of the dyeing, another sample (sample 3 = 1 ml of dyebath after the dyeing process) was collected and the fabrics were removed from the dyebath and transferred to an extract bath containing dimethylformamide (DMF) and water (1 : 1). After 12 h of shaking at room temperature the fabrics were taken, rinsed with water and dried. The extract bath was labelled as sample 4. All collected samples were diluted with water for accurate measurements of the absorbances (samples 1 and 2 were diluted 20-fold, sample 3 10-fold, sample 4 5-fold).

The primary and secondary exhaustion were calculated from the absorbance ratios at the dyes'  $\lambda_{\max}$  value of sample 2 and sample 1 (primary exhaustion) or sample 3 and sample 1 (secondary exhaustion), respectively. The fixation yield was determined by subtracting the amount of unfixed dye from the secondary exhaustion. This information was obtained from the absorbance of the extract bath (changes in the absorbance due to the presence of DMF were considered by introducing an empirical factor  $f_{\text{DMF/water}} = E_{\text{water}}/E_{\text{DMF/water}}$ ).

### 2.3 pKa values

The pH dependence of the absorption spectra (Fig. 1) in dilute aqueous solution ( $5 \times 10^{-5}$  mol/l, 22°C) was used to determine the pKa values of the dyes (dissociation of the *ortho*-hydroxyazo-proton or hydrazone NH-proton, respectively).

Due to the alkaline sensitivity of the VS reactive dyes, the hydroxy-

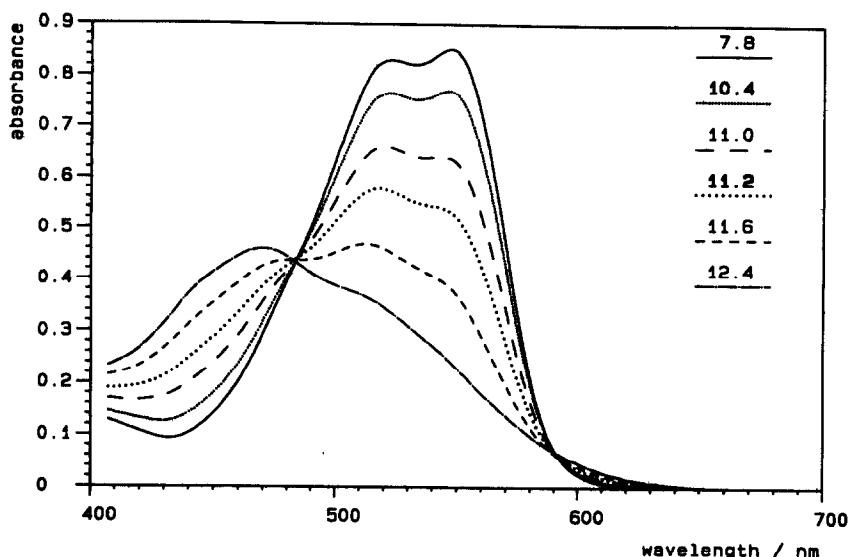


Fig. 1. VIS spectra of 3 (HES/MCT) at different pH values at  $[Dye] = 5 \times 10^{-5}$  mol/litre in water at 22°C.

ethylsulphone (HES)/MCT dyes were investigated. These dyes were prepared by coupling the diazonium salts on H-acid condensed with cyanuric chloride and *p*-( $\beta$ -hydroxyethyl)sulphonylaniline. This method yields pure HES/MCT dyes, compared to the hydrolysis of VS/MCT, which also yields HES/monohydroxytriazine (MHT).

To a solution of the dyestuff (400 ml) was added 50 mg of sodium bicarbonate to buffer against further alkali addition. This solution was titrated with 1 N NaOH. The spectrum was measured after each alkali addition by pumping the solution into a flow cell connected to the Perkin Elmer spectrophotometer (Perkin Elmer & Co, Überlingen, Germany). The current pH value was measured continuously with a pH electrode. After addition of 2.5 ml of NaOH solution, solid NaOH was added to avoid concentration changes caused by dilution. For solutions at very high pH values (pH >12.5) a different approach was applied due to the inaccuracy in pH measurements with the pH electrode. In those cases the solutions were freshly prepared, e.g. with Merck buffer solution of pH 13.

To calculate  $pK_a$  values from the obtained spectral data the procedure was as follows: the additivity of the spectra of the dissociated ( $D^-$ ) and the undissociated dye (HD) can be assumed if isosbestic points are present (Fig. 1). Thus, one may write for the absorbance ( $E$ ) at a given pH value and wavelength:

$$E = x_{HD} \cdot E_{O,HD} + x_{D^-} \cdot E_{O,D^-} \quad (1)$$

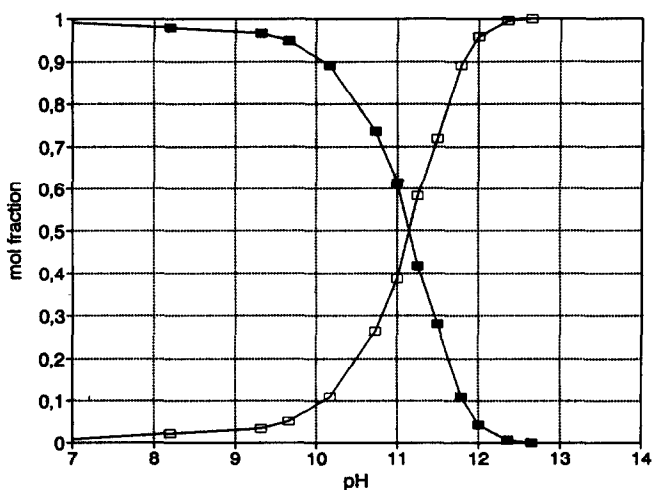


Fig. 2. Mole fractions of dye 3 plotted versus the pH value for the dissociated dye  $D^-$  (□) and the undissociated dye HD (■).

where  $x_{HD}$  and  $x_{D^-}$  are the mole fractions of HD and  $D^-$ , respectively and  $E_o$  are absorbance values of the pure forms HD and  $D^-$ . They can be measured at the extreme pH values, e.g.  $E_{o,HD}$  at pH 7 and  $E_{o,D^-}$  at pH 13. Also, with only two species present we can write  $x_{D^-} = 1 - x_{HD}$ . Thus, eqn (1) may be transformed into

$$x_{HD} = \frac{E - E_{o,D^-}}{E_{o,HD} - E_{o,D^-}} \quad (2)$$

The fractions  $x_{HD}$  and  $x_{D^-}$  were calculated according to eqn (2) at a given wavelength ( $\lambda_{max}$  of HD) and plotted versus pH (Fig. 2). The pKa value was then determined graphically at  $x_{D^-} = x_{HD} = 0.5$ .

## 2.4 Aggregation

The visible (VIS) absorption spectra of the chromatographically purified dyes were measured with a Perkin Elmer Lambda 2 spectrophotometer. In the case of double-band absorption spectra only the absorbance at the higher wavelength was considered for the evaluation of the absorption coefficients.

The applied media for the measurements and absorption coefficient determinations were water ( $\epsilon_{water}$ ), water containing 25 g/litre sodium sulphate ( $\epsilon_{salt}$ ), water containing 10% dimethylacetamide ( $\epsilon_{DMA}$ ) at a dye concentration of  $5 \times 10^{-5}$  mol/litre and water at a 20 times higher concentration ( $10^{-3}$  mol/litre,  $\epsilon_{conc}$ ). All these spectra were measured at 22°C.

In addition, data at 0°C ( $\epsilon_{ice}$ ) and 60°C ( $\epsilon_{60}$ ) were collected ( $5 \times 10^{-5}$  mol/litre, water).

The ratio of the  $\epsilon$  value in a given medium to the reference system ( $\epsilon_{water}$  was used as reference system) is defined as aggregation parameter  $\phi_i$ :

$$\phi_i = \frac{\epsilon_{\lambda_{max},i}}{\epsilon_{\lambda_{max},water}} \quad (3)$$

In each case the wavelength of the maximum absorbance ( $\lambda_{max}$ ) under the applied conditions was used. With this procedure any deviations caused by bathochromic or hypsochromic shifts were taken into account.

In order to establish more clearly the differences between the dyes a total aggregation parameter was defined (parameters favouring aggregation stand in the nominator, the others in the denominator; the parameters  $\phi_{ice}$  and  $\phi_{60}$  were not considered here because they have no significant effect):

$$\Phi_{tot} = \frac{\phi_{salt} \cdot \phi_{conc}}{\phi_{DMA}} \quad (4)$$

### 3 RESULTS AND DISCUSSION

#### 3.1 Characterization of the dyes by VIS spectroscopy and NMR spectroscopy—discussion of azo-hydrazone tautomerism and linear free energy relationships

Table 3 gives spectral data for the dyes, the wavelength of maximum absorbance ( $\lambda_{max}$ ) and the molar extinction coefficients ( $\epsilon$ ). Electron donating substituents significantly influence the colour, causing a bathochromic shift of  $\lambda_{max}$  while electron withdrawing substituents do not significantly affect  $\lambda_{max}$  (see series 1–5 in Table 3).

Hydroxyazo type dyes are charge transfer (CT) chromophores, and the influence of substituents on the light absorption is well understood.<sup>5</sup> Basically, if one plots the wavelength of maximum absorbance versus Hammett's constants two separate straight line correlations are obtained and one can decide from the slope of the Hammett plot whether the hydrazone or the azo structure dominates ( $\delta_+ < 0/\delta_- \approx 0$  for the hydrazone and  $\delta_+ \approx 0/\delta_- > 0$  for the azo isomer; the index '+' stands for electron donating substituents and the index '-' for electron withdrawing ones). For the hydrazone form the diazo component is the donor part while it is the acceptor part for the azo form.

The dyes with identical substituents varying only in the position of



TABLE 3

Wavelength of Maximum Absorption and Extinction Coefficients of the Dyestuffs 1–12 in Water (pH 7, 22°C)

Dye	Type of absorption band <sup>a</sup>	$\lambda_{\max}$ (nm)	$\epsilon \times 10^4$ ( $l \text{ mol}^{-1} \text{ cm}^{-1}$ )
1	d	538, 562	3.38
2	d	524, 550	3.34
3	d	518, 541	3.30
4	d	522, 543	3.24
5	s <sup>b</sup>	536 <sup>b</sup>	3.21
6	d	537, 564	3.16
7	d	527, 553	3.07
8	d	521, 543	2.95
9	ss <sup>c</sup>	534 <sup>c</sup>	2.49
10	d	514, 532	3.14
11	d	524, 550	3.14
12	d	513, 543	3.24

<sup>a</sup> s—singlet; d—doublet; ss—singlet with shoulder.<sup>b</sup> The band appears as a singlet. However, this is accidental and splitting occurs by the addition of either salt or DMA, leading to a doublet (Fig. 4). The  $\lambda_{\max}$  values are 522 and 545 nm when the slight bathochromic shifts caused by the additives are considered.<sup>c</sup> Same as *b*. Splitting into two bands at 520 and 543 nm.

attachment, either *ortho* or *para* to the azo group (the pairs 1/6, 2/7, 4/8 and 5/9) have almost identical  $\lambda_{\max}$  values (Table 3). Thus, it is reasonable to include both *ortho* and *para* substituted dyes in the Hammett plot (Fig. 3). Mustroph used, in a similar approach, absorbance increments for estimating previously unknown Hammett  $\sigma$ -values of *ortho* substituents.<sup>6,7</sup> All dyes except for 10, which is significantly more hypsochromic than expected, follow fairly well the anticipated correlation (Fig. 3). Indeed, there are two straight lines with remarkably different slopes as expected for CT chromophores. The observed Hammett dependence of the  $\lambda_{\max}$  (see above) is only consistent with the hydrazone form, and the inverse case would be expected for the azo isomer.<sup>5</sup> In a former work, an analogous Hammett correlation was also found for other *ortho*-hydroxyazo dyes based on 1-naphthol-4-sulphonic acid as coupling component.<sup>8</sup>

The phenomenon of azo-hydrazone tautomerism has been the subject of much research and is well documented in the literature, e.g. in a review by Ball and Nicholls.<sup>9</sup> Either one of the two isomers may dominate, depending on the chemical constitution of the dyestuffs. According to <sup>13</sup>C-NMR spectra, the hydrazone configuration very strongly prevails for *ortho*-hydroxyazo dyes based on H-acid.<sup>10,11</sup> The chemical shift values

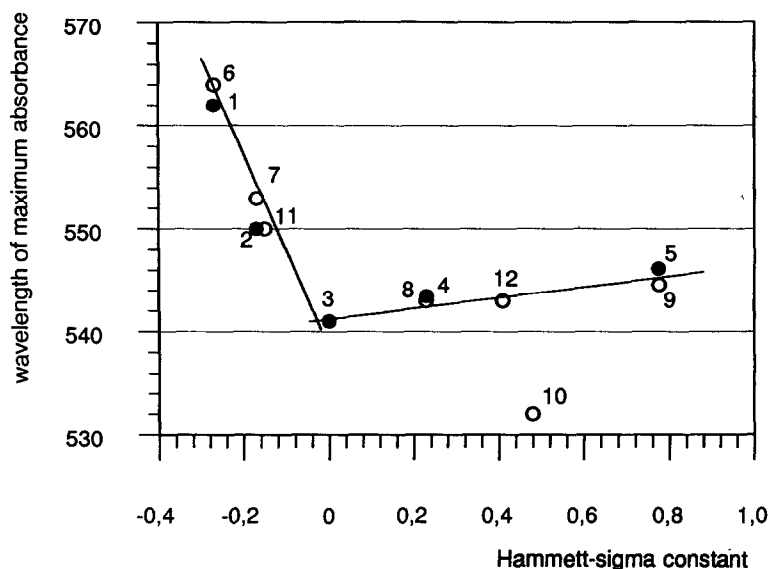
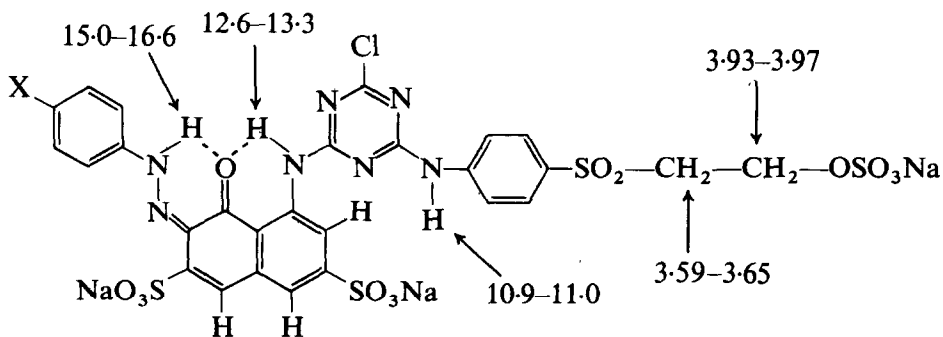


Fig. 3. Hammett plot for the wavelength of maximum absorbance for both *para* (●) and *ortho* (○) substituted dyes 1–12.

of the carbonyl  $^{13}\text{C}$ -NMR signal of the hydrazone tautomer is shifted much further downfield than the corresponding  $^{13}\text{C}$ -NMR signal of the aromatic carbon of the hydroxyazo tautomer.<sup>10</sup> For the corresponding *para*-hydroxyazo dyes and the *ortho*-aminoazo dyes, however, the azo tautomers prevail.<sup>11</sup> The stabilizing effect of intramolecular hydrogen bonding was made responsible for the dominance of the hydrazone tautomer in the case of the *ortho*-hydroxyazo dyes.<sup>9</sup>

The key  $^1\text{H}$ -NMR chemical shifts (ppm) of the dyestuffs that were investigated in this work can be assigned as follows (see Table 2):



The  $^1\text{H}$ -NMR signal of the corresponding hydrazone proton is shifted downfield to remarkable values higher than 15 ppm. This indicates very strong hydrogen bonds. Besides, the chemical shifts of the other proton

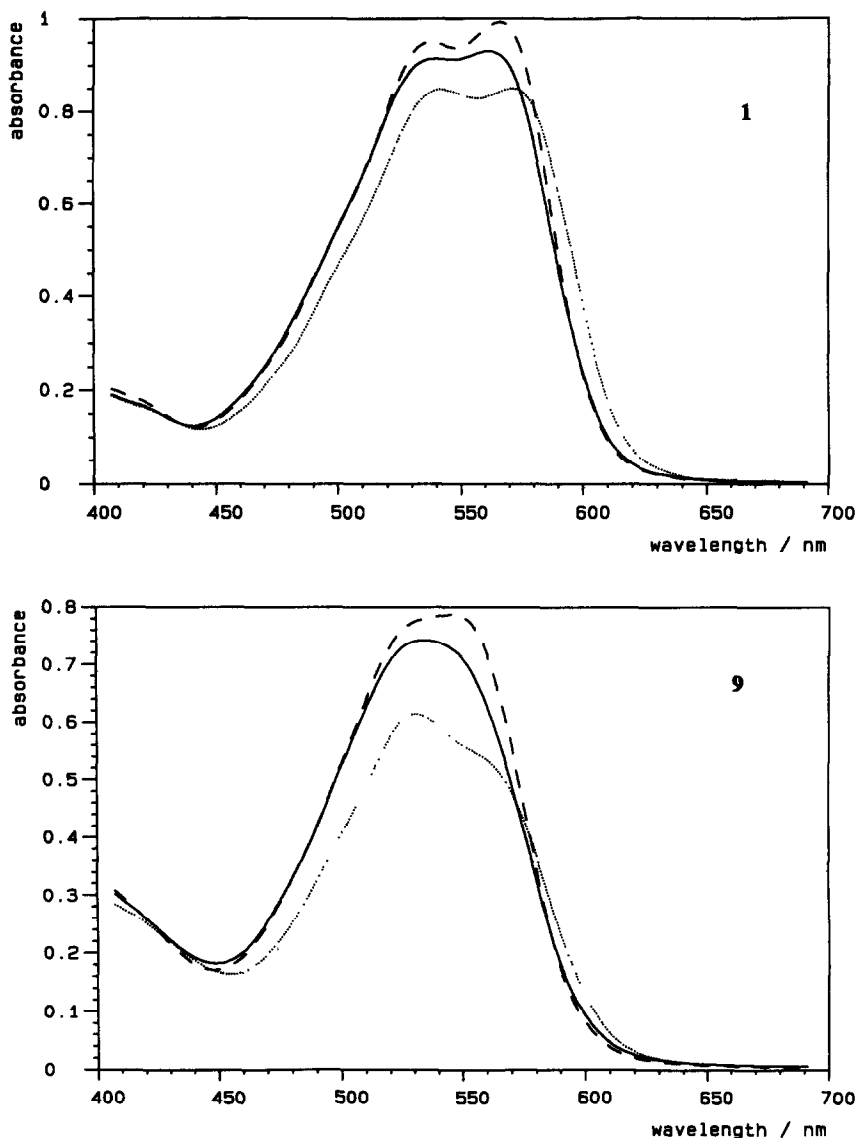


Fig. 4. VIS spectra of 1 and 9 (SES/MCT) at  $[Dye] = 5 \times 10^{-5}$  mol/litre in water (—), water containing 25 g/litre  $Na_2SO_4$  (.....) and water containing 10% DMA (---), at pH 7 and 22°C.

attached to the N atom of the H-acid fragment is also shifted downfield to *c.* 13 ppm. Thus, one may regard the H-acid type of dyes as a complex system where two hydrogen bonds are involved via planar six-membered rings. There may even be a third hydrogen bond when a suitable substituent in the *ortho* position to the azo linkage is present to give a bifurcated hydrogen bond to the hydrazone NH proton (see

Section 3.3). The shared bifurcated hydrogen bond tends to hold the phenyl ring of the diazo moiety in the same plane as the naphthalene ring of the coupling component, as was demonstrated by X-ray crystal structure determination of azo pigments, in the case of an *ortho*-nitro substituent.<sup>12</sup>

For all dyes a strong doublet appears in the VIS absorbance spectrum (Fig. 4, Table 3). Yet there is no significant content of the azo isomer and, therefore, the question arises as to the origin of the two bands. There is some work published concerning the appearance of doublets in VIS spectra, e.g. Haessner *et al.*<sup>13</sup> separated overlapping absorption bands by a mathematical analysis and attributed two bands to the hydrazone isomer alone. Dehari *et al.*<sup>14</sup> also reported on hydrazone doublets. According to MO (molecular orbital theory) based theoretical arguments, it may very well be due to two separate electronic excitations.<sup>15</sup> In addition, two closely neighboured absorption bands were interpreted as monomer and dimer bands of the dyes.<sup>16</sup> If this theory is valid here also, dye aggregation would definitely have an effect on the shape of the absorption spectra. The possible effect of dye aggregation will be discussed later (Section 3.3). Furthermore, it is very likely that the lower  $\epsilon$ -value of some dyes in water (especially **9**) is due to aggregation (Section 3.3, Table 3).

The NMR chemical shift values plotted versus the Hammett  $\sigma$ -constant for the *para* series (**1**–**5**) demonstrates the substituent effect on the NMR chemical shift (Fig. 5). Again, in accord with the above arguments, the highest value for **1** demonstrates that a remarkable azo content of this compound is improbable since the chemical shift of an azo compound is supposed to appear much further upfield. Electron donating substituents cause downfield shifts, possibly by their influence on the hydrogen bond stability. The same dependence has also been established for other azo dyes in the hydrazone form.<sup>17</sup>

### 3.2 pKa values

pKa values of *ortho*-hydroxyazo dyes have been reported by Zollinger.<sup>4</sup> This present paper broadly confirms his results for the H-acid dyes (with *para* substituents in the diazo moiety). In addition, corresponding data for *ortho*-substituted dyes are discussed and evaluated.

The dissociation of OH and NH functional groups in the dye molecule is an important feature for solubility and substantivity during the dyeing process, the reactivity of fibre reactive groups and also for the stability towards oxidative degradation as will be reported later (Part II in this series).

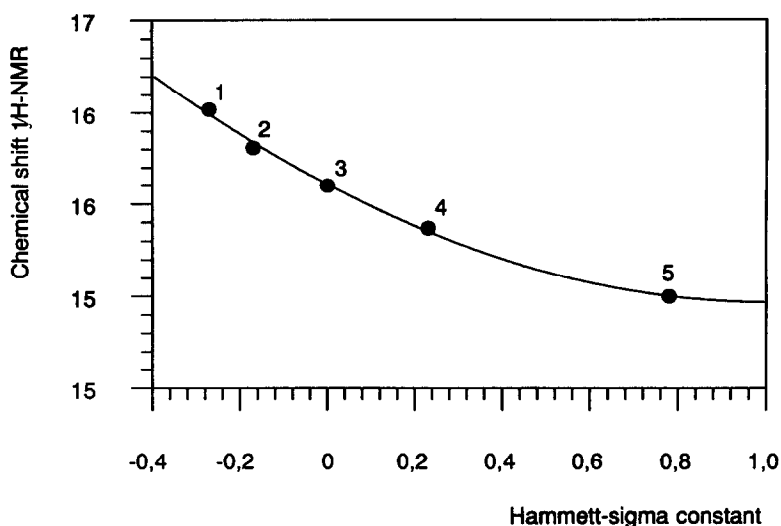


Fig. 5.  $^1\text{H}$ -NMR chemical shift value (250 MHz FT-NMR,  $\text{d}_6$ -DMSO) of the hydrazone NH signal plotted versus Hammett constant for the *para*-substituted dyes 1–5.

Several effects of substituents in the dye molecule have to be considered. Electronic effects may stabilize the dissociated dye anion by mesomeric or inductive effects. Steric restraints may hinder the attack of an incoming base required for the deprotonation. In addition, hydrogen bonding from *ortho* substituents to the hydrazone NH-proton should also increase the  $\text{pK}_a$  value. The series of dyes with *para* substituents (1–5) is not affected by steric effects or hydrogen bonding to the substituents and therefore it only shows the electronic effect. A comparison of *ortho* with the corresponding *para* substituents signifies the additional steric and hydrogen bonding effects. The possible hydrogen bonding to *ortho* substituents for methoxy, nitro and carboxy has been suggested by Gordon and Gregory.<sup>18</sup> Furthermore, hydrogen bonding for *ortho* located nitro groups has been confirmed by X-ray crystal structure determination of some azo pigments.<sup>19</sup>

The NH group of the hydrazone isomer is fairly acidic and is supposed to deprotonate first. Only at very high pH values, above 13, does a second dissociation, probably due to the NH group of the H-acid bearing an MCT fragment,<sup>20</sup> need to be considered, since then deviations from the isosbestic point in the VIS spectra are observed. Slight inaccuracies in the determination of  $\text{pK}_a$  values for the dyes with very low acidity (9 and 12) cannot be excluded.

In general, the acidity of the NH of the hydrazone and the OH of the azo isomer is different. Only an effective  $\text{pK}_a$  value of the equilibrium

mixture can be measured. According to Section 3.1 the hydrazone tautomer strongly prevails, however.

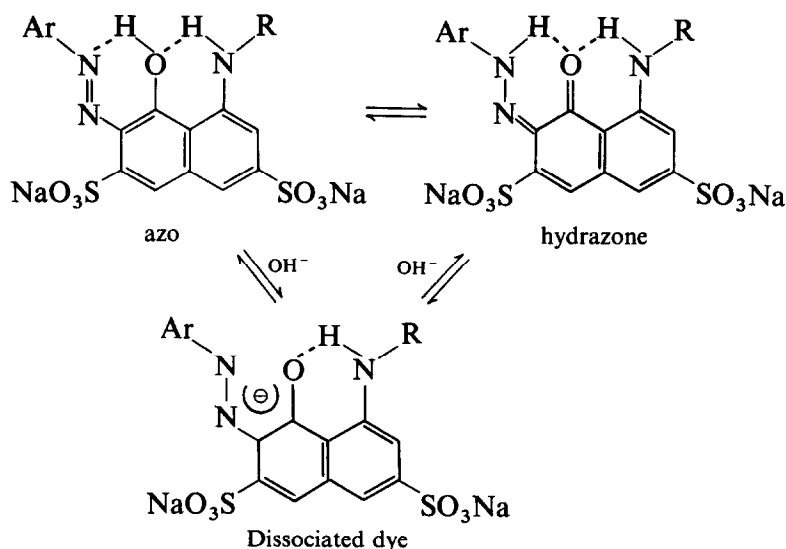


Table 4 illustrates the determined  $pK_a$  values for the 12 dyes. In the series of *para*-substituted dyes (1–5) a significant increase of the acidity (lower  $pK_a$  value), with electron withdrawing power of the substituents, is encountered. Only dye 1 (*p*-OCH<sub>3</sub>) shows a deviation from this observation. In a similar case this was explained with a higher azo content of the methoxy dye in comparison with the other dyes that should be widely hydrazone dyes.<sup>4</sup> On the other hand, the NMR data do not underline this suggestion, because dye 1 has the highest chemical shift in the series of *para*-substituted dyes (see Section 3.1).

Comparison of the *o*-methyl and *o*-chlorine dyes 7 and 8 with the

**TABLE 4**  
 $pK_a$  Values ( $\pm 0.1$ ) of the Dyestuffs 1–12 (HES/MCT)

<i>Substituent</i>	$pK_{a_{para}}$	$pK_{a_{ortho}}$	$\Delta pK_a$
OCH <sub>3</sub>	10.96 (1)	11.03 (6)	0.07
CH <sub>3</sub>	11.22 (2)	11.94 (7)	0.72
H	11.15 (3)	11.15 (3)	0
Cl	10.72 (4)	11.53 (8)	0.81
NO <sub>2</sub>	10.53 (5)	12.26 (9)	1.73
SO <sub>3</sub> H	—	11.74 (10)	—
<i>s</i> -C <sub>4</sub> H <sub>9</sub>	—	11.64 (11)	—
COOH	—	12.93 (12)	—

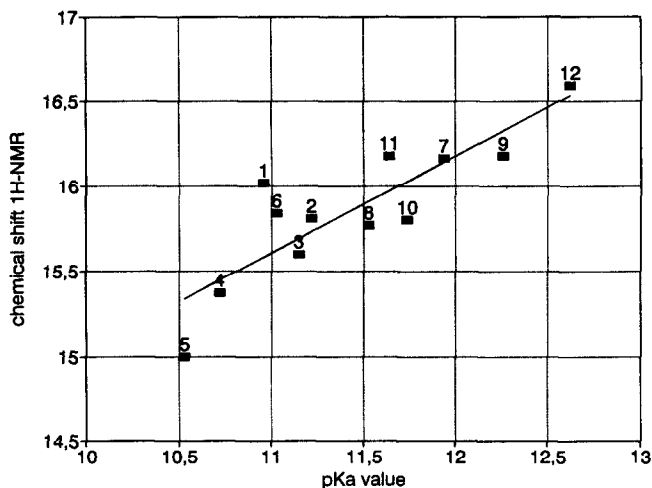


Fig. 6. <sup>1</sup>H-NMR chemical shift value (250 MHz FT-NMR, d<sub>6</sub>-DMSO) of the hydrazone NH signal plotted versus the pK<sub>a</sub> value for the corresponding dye 1–12 (correlation coefficient 0.8587; standard deviation 0.226).

corresponding *para*-substituted dyes 2 and 4 illustrates the steric effect on the pK<sub>a</sub> value. The pK<sub>a</sub> value of the *ortho* dye is enhanced by 0.72 and 0.81, respectively.

Surprisingly, the pK<sub>a</sub> values of 10 and 11 are lower than expected, based on the steric requirements of those rather bulky substituents (especially in comparison with 7). One possible explanation is a twist of the diazo moiety out of the plane formed by the H-acid–MCT system. In this case the steric restraints of *ortho*-located substituents would be lower than expected.

Very surprisingly, no significant difference in the pK<sub>a</sub> values of 1 and 6, *para*- and *ortho*-methoxy, is encountered. Thus, any hydrogen bonding can be excluded in the case of the *ortho*-methoxy substituent. Dyes 9 and 12 have extremely high pK<sub>a</sub> values which can only be explained by additional stabilizing of the undissociated dyes caused by intramolecular hydrogen bonding from the *ortho* substituent to the hydrazone proton.

In the case of the least acidic dye 12 containing an *ortho*-carboxy substituent, its NMR chemical shift value is shifted further downfield to 16.6 ppm (Table 2). Apparently, the NMR signal of the rather acidic hydrazone proton can be connected to a certain degree with pK<sub>a</sub> values (Fig. 6). There is still a substantial deviation from a straight line correlation for some dyes, indicating some other effects. A similar correlation has also been described for other dyes.<sup>17</sup>

Sometimes correlations between certain dyeing parameters, e.g. aggregation and substantivity or substantivity and fixation yields, yield only very

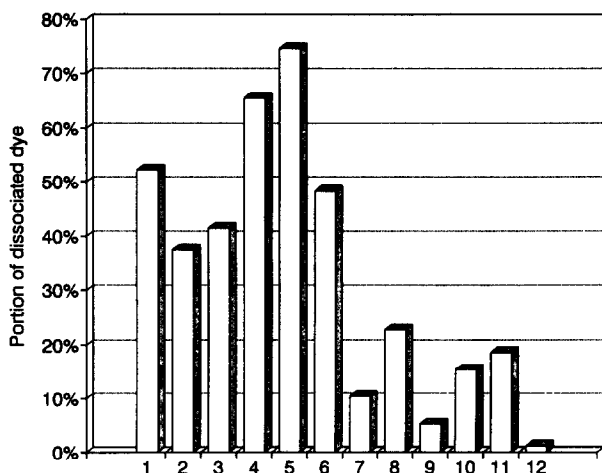


Fig. 7. Portion (%) of dissociated hydroxyazo group of the dyes 1–12 at pH 11.

unsatisfying results.<sup>21</sup> This may be explained with the dye dissociation. Substantivity is frequently measured at neutral pH values, while the dyeing is performed in alkaline medium. Especially the dye aggregation may be affected strongly because an additional anionic charge is introduced by the dissociation process. The fraction of the dissociated hydroxyazo group in the dye molecule at pH 11 (pH of exhaustion dyeing process) depends largely on the substitution pattern, as can be seen in Fig. 7.

### 3.3 Dye aggregation

Many different methods have been introduced in the literature to describe dye aggregation, e.g. measurements of the osmotic pressure and conductivity,<sup>22</sup> quasi elastic light scattering,<sup>23</sup> diffusion methods,<sup>24</sup> analysis of absorption spectra<sup>25–27</sup> and, recently, small angle X-ray scattering.<sup>28</sup> Here a new method is introduced to assess dye aggregation by evaluation of the absorption spectra under defined conditions. Basically, we use deviations from the Lambert–Beer law of absorbance. This rather simple approach uses very easily obtainable spectral data and can be conducted in a very short period of time.

High dye concentrations, high salt contents and low temperature are factors that tend to favour the aggregation of dyestuff molecules. In contrast, the addition of hydrotropic substances (alcohols, dimethylacetamide, acetonitrile, urea, etc.) diminish the tendency of the dyes to aggregate. The aggregation parameter  $\phi$  (see Section 2.4) considers the influence of such factors on the absorbance. Generally,  $\phi > 1$  means the absorbance is enhanced (decrease in aggregation) due to the action of



**TABLE 5**  
Aggregation Parameters  $\phi_i$  ( $\pm 0.01$ ) and  $\Phi_{\text{tot}}$  ( $\pm 0.02$ ) of the Dyestuffs 1–12

Dye	$\phi_{\text{DMA}}$	$\phi_{\text{salt}}$	$\phi_{\text{conc}}$	$\phi_{\text{ice}}$	$\phi_{60}^a$	$\Phi_{\text{tot}}$
1	1.05	0.90	0.94	0.99	0.99	0.81
2	1.05	0.89	0.94	1.00	0.98	0.80
3	1.04	0.89	0.94	0.99	0.98	0.80
4	1.06	0.88	0.94	0.98	0.99	0.78
5	1.08	0.85	0.89	0.94	1.00	0.70
6	1.05	0.90	0.93	0.97	0.98	0.80
7	1.08	0.84	0.91	0.96	0.98	0.71
8	1.04	0.81	0.90	0.95	0.99	0.70
9	1.08	0.73	0.84	0.93	1.04	0.57
10	1.02	1.00	1.00	1.03	0.98	0.98
11	1.05	0.83	0.92	0.98	0.98	0.73
12	1.00	0.94	1.01	1.02	0.98	0.95

<sup>a</sup> Due to the thermic expansion we suggest that  $\phi_{60} = 0.98$  corresponds to no changes in the physical state.

additives, and reversely,  $\phi < 1$  means a decrease in absorbance (increase in aggregation).  $\phi_{\text{DMA}} > 1$  means the dye is already aggregated in dilute aqueous solution, because otherwise the absorbance would not be expected to rise upon the addition of DMA. On the other hand,  $\phi_{\text{salt}} < 1$  signifies an increase in aggregation due to salt addition. This aspect is also very important with respect to dyeing. Parameters  $\phi_{\text{ice}}$  and  $\phi_{60}$  demonstrate the temperature dependence upon dye aggregation. Finally,  $\phi_{\text{conc}}$  shows the effect of increasing dye concentration on aggregation.

Table 5 contains the obtained aggregation parameters. It is immediately evident that most dyes aggregate strongly even in dilute solution ( $\phi_{\text{DMA}} > 1$ ). The aggregation can be enhanced by the addition of salt ( $\phi_{\text{salt}} < 1$ ) and by increasing the concentration of the dyes ( $\phi_{\text{conc}} < 1$ ). Changes in  $\phi$  values with temperature variations are small and negligible in most cases, except for dye 9.

Dyes 10 and 12 have  $\phi$  values near 1. This suggests that they do not aggregate to a considerable extent under the conditions applied here. The additional anionic charge ( $\text{COO}^-$ ,  $\text{SO}_3^-$ ) in the dye molecule possibly increases the solubility and lowers the aggregation behaviour.

Aggregation is enhanced with the electron withdrawing power of the substituents. This observation holds for both the *para* series (1–5) and for the *ortho* series (6–9). Parameters  $\phi_{\text{salt}}$ ,  $\phi_{\text{DMA}}$ ,  $\phi_{\text{conc}}$ , and particularly  $\Phi_{\text{tot}}$  (Fig. 8) clearly underline this suggestion. Furthermore, comparison of isomeric dyes (*ortho* and *para*) reveals that the *ortho*-substituted dyes aggregate stronger than the *para*-substituted dyes. Dye 9 (*o*-nitro)

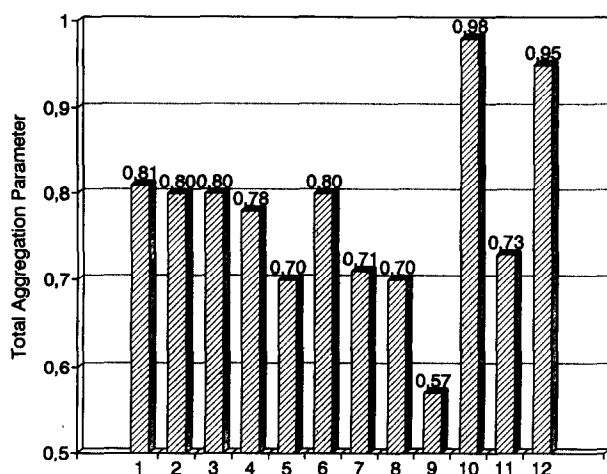


Fig. 8. Total aggregation parameter  $\Phi_{\text{tot}}$  ( $\pm 0.02$ ) for the 1–12 dyes.

is the dye with the strongest aggregation behaviour in this series ( $\Phi_{\text{tot}} = 0.57$ ).

Dyes based on H-acid very often appear as a doublet in the VIS spectrum (Fig. 4). The phenomenon of double-band shaped absorption spectra is encountered in many other cases as well, e.g. for triphenyl-methane dyes.<sup>16,29</sup> Förster and König explained this with monomeric and sandwich-like dimeric absorption bands.<sup>16</sup> The absorption at the higher wavelength was assigned to the dye monomer and the other to the dimer.

TABLE 6

Dyeing Properties of Dyes 1–12 on Cotton Fabric (2% o.w.f., liquor ratio 1 : 20, at 60°C isothermic, 60 min primary exhaustion with 50 g/litre sodium chloride; 90 min secondary exhaustion with 20 g/litre sodium carbonate)

Dye	Primary exhaustion (%)	Secondary exhaustion (%)	Fixation yield (%)	Relative fixation yield (%)
1	54	86	67	78
2	50	87	64	74
3	41	83	64	77
4	62	87	65	75
5	73	81	61	75
6	51	86	67	77
7	58	90	69	76
8	49	87	66	76
9	35	69	49	77
10	20	69	61	88
11	51	75	38	50
12	47	84	75	89

Based on this assumption, some research has been carried out on azo dyes based on H-acid as well.<sup>25,30</sup> If only two species (monomer and dimer) are present, a concentration dependent or temperature dependent isosbestic point is observed.<sup>16</sup> However, for the dyes discussed here this is definitely not the case. Therefore, either the existence of larger aggregates must be assumed or the assumption of dimer absorbance ought to be rejected in this particular case.

The absorption band at the lower wavelength gains some intensity relative to the one at the higher wavelength if one changes the medium towards an aggregation favouring environment (DMA  $\rightarrow$  water  $\rightarrow$  salt). Theoretically, the relative shift of intensities would be consistent with the theory of monomeric and dimeric structural fragments in higher aggregates being responsible for the appearance of two absorption bands. However, this effect is very small for most dyes and it still remains unresolved why even the weakly aggregating dyes **10** and **12** exhibit double bands at all (see Section 3.1, Table 3), and thus a critical attitude must be adopted towards this interpretation.

### 3.4 Dyeing behaviour

The results obtained on the exhaustion dyeing for the applied dyestuffs in this series are recorded in Table 6. The fixation yields range between 60 and 70% except for the dyes **9** and **11** whose yield is significantly lower, and dye **12**, which achieves a higher yield of 75%. The relative fixation yield is higher than 70% for all dyes, except for **11** (50%). Dyes **10** and **12** especially, have high relative yields, close to 90%. These two dyes aggregate to a lower degree than the others (see Section 3.3) and thus dye aggregation seems to be a limiting factor for the fixation process. Dye **9**, however, aggregates strongly and is yet not significantly affected in its relative fixation yield. The poor absolute yield may be related to its low substantivity (neutral exhaustion). Dye **10** has the poorest neutral exhaustion of all dyes, but this is compensated by the good relative fixation ratio. In general, the neutral exhaustion varies significantly, but this, in most cases, does not affect at all the secondary exhaustion. Most dyes have values higher than 80%. Apparently, the conditions in phase 1 (neutral pH) cannot be compared with those in phase 2 (alkaline pH) due to several changes. SES is converted into VS, and the loss of ionic charge may affect the dye's aggregation and substantivity. The fixation process not only removes some of the dye content from the dyebath's exhaustion equilibrium, but it also may change the substantivity as well (some dyes may tend to adsorb at sites where already others are). Also, the effect of proton dissociation mentioned above needs to be considered.

## ACKNOWLEDGMENTS

C.S. expresses his gratitude to the Stipendienfonds der Chemischen Industrie, Frankfurt am Main, for financial support. We specially thank Dr H. Tappe and Dr W. Russ, of Hoechst AG, Frankfurt am Main, for their fruitful suggestions during this work.

## REFERENCES

1. Schumacher, C., Ph.D. Thesis, Universität Stuttgart, Germany 1992.
2. Abeta, S., Yoshida, T. & Imada, K., *Am. Dyest. Rep.*, **73**(7) (1984) 26.
3. Fierz-David, H. E. & Matter, M., *J. Soc. Dyers Colour.*, **53** (1937) 424.
4. Zollinger, H., *Chemie der Azofarbstoffe*, Birkhäuser, Basel, Switzerland, 1958. pp. 21–44, 111–76.
5. Mustroph, H., *J. Prakt. Chem.*, **327** (1985) 121.
6. Mustroph, H. & Epperlein, J., *J. Prakt. Chem.*, **322** (1980) 49.
7. Mustroph, H., *Z. Chem.*, **25** (1985) 385.
8. Suzuki, S., Das, R. C., Harada, K. & Stoyanov, S., *Bull. Chem. Soc. Jpn.*, **53** (1980) 2666.
9. Ball, P. & Nicholls, C. H., *Dyes and Pigments*, **3** (1982) 5.
10. Lycka, A. & Jirman, J., *Dyes and Pigments*, **8** (1987) 315.
11. Fedorow, L. A., Sokolovskii, S. A. & Dvoskin, S. I., *J. Anal. Chem. USSR*, **42** (1988) 1390.
12. Whitaker, J. *Soc. Dyers Colour.*, **94** (1978) 431.
13. Haessner, R., Mustroph, H. & Borsdorff, P., *Dyes and Pigments*, **6** (1985) 277.
14. Dehari, C., Mutsunaga, Y. & Tani, K., *Bull. Chem. Soc. Jpn.*, **43** (1970), 3404.
15. Simov, D. & Stojanov, S., *J. Mol. Struct.*, **19** (1973) 255.
16. Förster, T. & König, E., *Z. Elektrochem.*, **61** (1957) 344.
17. Kettrup, A., Groethe, M. & Hartmann, J., *Monatsh. Chem.*, **107** (1976) 1391.
18. Gordon, P. F. & Gregory, P., *Organic Chemistry in Colour*, Springer-Verlag, Berlin, 1983, pp. 100–105.
19. Whitaker, A., *Z. Kristallogr.*, **145** (1977) 271; **147** (1978) 99.
20. Ackermann, H. & Dussy, P., *Helv. Chim. Acta.*, **45** (1962) 1683.
21. Abeta, S., Akahori, K., Meyer, U. & Zollinger, H., *J. Soc. Dyers Colour.*, **107** (1991) 12.
22. Milicevic, B. & Eigenmann, B., *Helv. Chim. Acta.*, **47** (1964) 1039.
23. Chavan, R. B. & Venkata Rao, J., *J. Soc. Dyers Colour.*, **99** (1983) 126.
24. Klimenko, N. A., Lupashku, F. G., Koganovskii, A. M. & Ropot, V. M., *Colloid J. USSR, Engl. Transl.*, **41** (1979) 100.
25. Weingarten, R., *Melliand Textilber.*, **48** (1967) 301.
26. Pugh, D., Giles, C. H. & Duff, D. G., *Trans. Faraday Soc.*, **67** (1971) 563.
27. Baumgarte, U., *Textilveredlung*, **15** (1980) 413.
28. Harada, M., Akahori, K., Imada, K., Abeta, S., Tanimura, H., Urakawa, H., Kajiwara, K. & Ito, T., *11. Int. Farbensymposium*, Montreux, Switzerland,

23–26 September 1991. Schweizerischer Chemiker-Verband (SChV), Schweizerische Chemische Gesellschaft (SCG), Gesellschaft Deutscher Chemiker (GDEG).

29. Valdes-Aguilera, O. & Neckers, D. C., *Acc. Chem. Res.*, **22** (1989) 171.
30. Fiebig, D., Herlinger, H., Stini, H. L. & Kruspel, G., *Melliand Textilber.*, **71** (1990) 460.